Ge-H empirical potential and simulation of Si epitaxy on Ge(100) by chemical vapor deposition from SiH_4

L. Yang,[1,2] G. Pourtois,[1] M. Caymax,[1] A. Ceulemans,[2] and M. Heyns[1,3]
[1]*IMEC, Kapeldreef 75, B-3001 Leuven, Belgium*
[2]*Department of Chemistry and INPAC Institute, University of Leuven, B-3001 Leuven, Belgium*
[3]*Department of Electrical Engineering, University of Leuven, B-3001 Leuven, Belgium*
(Received 22 September 2008; revised manuscript received 27 January 2009; published 16 April 2009)

A parameter set describing the Ge-H bonds in the framework of the many-body interatomic potential proposed by Tersoff and Murty has been derived using first-principles calculations. The potential was fitted to reproduce structural, energetic, and vibration properties of gas phase germanium hydrides and radicals. It demonstrates a good transferability for the description of hydrogen terminated germanium surfaces. The potential has been used to simulate the epitaxial growth of a Si layer on a Ge(100) surface using SiH_4 precursor molecules. The obtained results faithfully reproduce the impact of chemisorbed hydrogen on the mechanism of Ge diffusion in the grown Si layer.

DOI: 10.1103/PhysRevB.79.165312 PACS number(s): 81.05.Cy, 81.15.Gh, 61.50.Ah

I. INTRODUCTION

Important research efforts are currently devoted to the investigation of high-mobility semiconductors for their potential applications in future high performance metal-oxide-semiconductor field effect transistors (MOSFET). Germanium is of particular interests[1–3] due to its high electron and hole mobility, which together with its low processing temperature, potentially enable its integration with high-κ gate dielectrics.

However, a major drawback to the application of Ge in MOS devices is the poor electrical quality of its native oxide compared to SiO_2, requiring a proper passivation of the Ge surface before the deposition of the gate dielectric to obtain low interface state densities and a high carrier mobility. In that respect, a promising route for the passivation of Ge consists in depositing an ultrathin (atomic) epitaxial Si layer on the surface, which is partly oxidized at low temperature prior to the deposition of the dielectric. Recently, very good performances were reported on *p*-MOSFETs with $Ge/Si/SiO_x/HfO_2/TaN$ gate stacks.[4,5] To be electrically efficient, the diffusion of germanium in the passivating layer has to be minimized during the chemical vapor deposition process (CVD). The mechanisms at the origin of the diffusion are still under investigation,[6–8] and require insights into the very nature of the film growth process to unlock them. Obviously, the chemistry of hydrogen, silicon, and germanium are key factors that govern the film growth. Many of the reaction processes involving the CVD precursors occur at a time scale and model size that are beyond the scope of first-principles approaches but which can be described by using classical molecular dynamic (MD) method combined with empirical force constants. While empirical potentials describing the Si-Si, Ge-Ge, Si-Ge, and Si-H interactions are well documented in literature,[9,10] a robust parametrization for the Ge-H potential is still missing. The development of a transferable parametrization for the Ge-H interaction is hence of prime importance to describe this deposition process.

The paper is organized as follows: we first briefly describe the form of the classical potential together with the fitting procedure used. We then review the parameters obtained and their transferability to finally study the CVD deposition of silicon atomic layer (AL) on a germanium substrate.

II. METHODOLOGY

A. Interaction potential

Previous attempts have been reported to derive an effective potential for the Ge-H bond. For instance, Ciobanu and Briggs[11] used the original Tersoff potential[9] to fit the Ge-H interactions. However, the original form of the Tersoff potential does not completely capture the complexity of the Ge-H bond and peculiarly its dependence on the chemical environment, which leads to an improper description of the radical forms of Ge hydrides. On the other hand, empirical potentials for Si-H have been extensively developed for many years.[10–12] Among them, the modified Tersoff potential developed by Murty and Atwater[10] has proven its transferability and accuracy, while keeping a rather simple analytical form. It faithfully describes a large amount of silane molecules together with their radical forms. In this paper, we extend the formalism developed by these authors to the Ge-H case. This approach has the advantage to be easily combinable with the original Tersoff empirical potential for the Ge-Ge, Si-Si, Si-Ge, Si-H interactions,[9,10] which allows a simple empirical description of the Ge-Si-H systems.

According to Murty and Atwater,[10] the total potential energy of a hydrogenated bond can be written as

$$E = \sum_i E_i = \frac{1}{2}\sum_{i\neq j} \Phi_{ij}, \tag{1}$$

$$\begin{aligned}\Phi_{ij} = \{&AF_1(N)\exp(-\lambda_1 r_{ij}) \\ &- B_0F_2(N)\exp(-\lambda_2 r_{ij})(1+\varsigma_{ij}^{\eta})^{-\delta}\}f_c(r_{ij}),\end{aligned}$$

$$\begin{aligned}\varsigma_{ij} = \sum_{k\neq i,j} &f_c(r_{ij})[c + d\{H(N) - \cos\,\theta_{jik}\}^2] \\ &\times \exp[\alpha\{(r_{ij}-R_{ij}^{(e)}) - (r_{ik}-R_{ik}^{(e)})\}^{\beta}],\end{aligned} \tag{2}$$

 ©2009 The American Physical Society

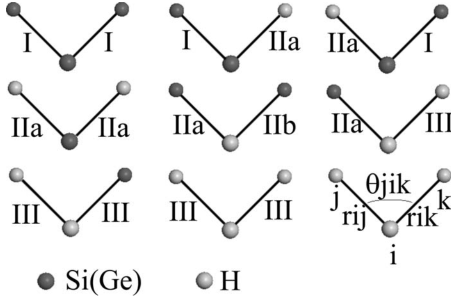

FIG. 1. Illustration of the different combination of interactions. For the sake of clarity, we used the same notations as the ones proposed in Ref. 9 and correspond to the parameter set listed in Table II.

$$N_H^{i=(\mathrm{Si,Ge})} = \sum_{j=(H)} f_c(r_{ij}), \quad N_{\mathrm{Si,Ge}}^{i=(\mathrm{Si,Ge})} = \sum_{j=(\mathrm{Si,Ge})} f_c(r_{ij}), \tag{3}$$

$$f_c(r_{ij}) = \begin{cases} 1, r_{ij} < R - D \\ 0.5 - 9/16 \sin\left[\pi \dfrac{r_{ij} - R}{2D}\right] - 1/16 \sin\left[3\pi \dfrac{r_{ij} - R}{2D}\right], \\ R - D < r_{ij} < R + D \\ 0, r_{ij} > R + D. \end{cases} \tag{4}$$

where N is the coordination number of the Ge(Si) atom Ge-H(Si-H), $f_c(r_{ij})$ is the cutoff function. F_1 and F_2 are applied only to the Ge-H(Si-H) bonds. The parameters are combined to describe the interactions met in hydrogenated semiconductors (as illustrated in Fig. 1). A single potential is enough to provide a reasonable description of the Ge-H bond, independently of the type of the neighboring atoms due to its localized nature. Note that the angular dependence of the potential developed by Murty and Atwater [Eq. (2)] is a simplified version of the original formulation proposed by Tersoff (denoted in the following by the $_T$ subscript). In the latter,[9] c_T is about 10^4 times larger than d_T (for both Si and Ge), which allows rewriting the angular term of the original form as

$$\beta_T\{1 + c_T^2/d_T^2 - c_T^2/[d_T^2 + (h_T - \cos(\theta_{jik})^2\ ]\} \approx c + d[h_T - \cos(\theta_{jik})], \tag{5}$$

with c and d equal to

$$d = \beta_T c_T^2 / d_T^4, \tag{6}$$

$$c = \beta_T \approx 0. \tag{7}$$

In this paper, the Si-Ge and Ge-Ge interaction of the original Tersoff's (Ref. 9) formulation was adapted to the potential developed by Murty and Atwater according to Eqs. (6) and (7).

B. Parametrization

The parametrization of the Ge-H interactions has been obtained by fitting the physical properties of Ge-H clusters generated at a density-functional theory (DFT) level using the B3LYP exchange-correlation functional.[13] All the Ge hydrides cohesive energies were corrected with the zero-point vibration energy and the spin multiplicities corresponding to the lowest energy states were adopted. The quality of our reference systems has been assessed by comparing the computed bond lengths and their associated frequencies to literature values[14–19] (Table I). They have been selected to reproduce the impact of the hybridization of the orbitals on the Ge-H bond, namely, the constant elongation of the bond when going from a sp^3 to a nonhybridized situation, as illustrated in Table I.

TABLE I. Comparisons between the values computed at the DFT and other high level calculations or experimental reports for the Ge-H bond length and vibrational frequencies.

	pcGamess	Reference
$GeH_4[\alpha_{\mathrm{Ge\text{-}H}}(\text{Å})]$	1.533	1.525[a]
$GeH_3[\alpha_{\mathrm{Ge\text{-}H}}(\text{Å})]$	1.540	1.533[b]
$GeH_2[\alpha_{\mathrm{Ge\text{-}H}}(\text{Å})]$	1.604	1.587[c]
$GeH[\alpha_{\mathrm{Ge\text{-}H}}(\text{Å})]$	1.604	1.589[d]
	828	819[e]
	933	931[e]
	2129	2106[e]
$GeH_4[v(\mathrm{cm}^{-1})]$	2146	2214[e]
	936	920[f]
$GeH_2[v(\mathrm{cm}^{-1})]$	1888	1887[f]
$GeH[v(\mathrm{cm}^{-1})]$	1922	1834[d]

[a]Reference 14.
[b]Reference 15.
[c]Reference 16.
[d]Reference 17.
[e]Reference 18.
[f]Reference 19.

A set of relevant H terminated surface and bulk interstitial hydrogen structures were also generated at the generalized gradient approximation (GGA) [Perdew-Burke-Ernzerhof (PBE)] exchange-correlation level, using periodic boundary conditions. We used a numerical atomic approximation as it is implemented in the SIESTA code,[20] where the core electrons are implicitly treated by using Trouillier-Martins pseudopotentials[21] with the following electronic configuration of the elements: H $1s^1$ and Ge [Ar $3s^2 3p^6 3d^{10}$] $4s^2 4p^2$, where the core configurations are shown in brackets. The basis sets were of the double zeta polarization (DZP) type, optimized using the simplex minimization procedure proposed by Junquera *et al.*[22] to reproduce the structural parameters, the electronic properties and the energetic of bulk Ge, H_2, and hydrogenated Ge clusters obtained within a classical plane-wave expansion formalism.[23] Finally, the bulk Ge lattice constant computed at the GGA level (5.76 Å) has been used to build the surface models. An energy cutoff of 3537.48 eV and a $6\times6\times1$ Monkhorst-Pack grid for the sampling of the Brillouin zone were adopted, which were tested to ensure the convergence of the system properties to $\sim$0.5 meV/atom. The position of the atoms has been relaxed until a convergence of the atomic forces of 10 meV/Å is reached.

We then employed a force matching method, in which a target function which accounts for the force, the cohesive

TABLE II. Fitted parameters for the Ge-H potential.

	Ge-Ge (I)	Ge-H (IIa)	Ge-H (IIb)	H-H (III)
A(eV)	1.7690×10^{3}	6.3525×10^{2}		8.007×10^{1}
B_0(eV)	4.1923×10^{2}	4.6400×10^{1}		3.138×10^{1}
λ_1(Å^{-1})	2.4451	3.7923		4.2075
λ_2(Å^{-1})	1.7047	1.4660		1.7956
α(Å^{-1} or Å^{-3})	0.0000	6.8708	3.00	3.00
β	3.0000	3.00	1.00	1.00
$R^{(e)}$(Å)	2.4530	1.5360	1.5360	0.74
c	0.0000	2.7508×10^{-3}	1.2800	4.00
d	1.702×10^{-1}	3.8211×10^{-1}	1.000	0.00
h	-4.3884×10^{-1}	See below $H(\ )$	-1.000	0.00
R(Å)	2.95	1.90	1.90	1.55
D(Å)	0.15	0.15	0.15	0.45
η	7.5627×10^{-1}	1.0000	1.000	1.00
δ	6.6110×10^{-1}	8.0469×10^{-1}	8.0469×10^{-1}	8.0469×10^{-1}
$F1(1)$		1.3590		
$F1(2)$		1.2562		
$F1(3)$		9.7203×10^{-1}		
$F1(4)$		1.0000		
$F2(1)$		1.0491		
$F2(2)$		1.1136		
$F2(3)$		9.5033×10^{-1}		
$F2(4)$		1.0000		
$H(1)$		-4.0000×10^{-2}		
$H(2)$		3.4727×10^{-2}		
$H(3)$		-4.2963×10^{-1}		
$H(4)$		-4.2871×10^{-1}		

energy and the phonon modes constraints has been minimized by a simulated annealing algorithm[24] to generate the parameters reported in Table II. The forces and energetic of the following optimized clusters: GeH, GeH_2, GeH_3, GeH_4, Ge_2H_4(GeH-GeH_3), Ge_2H_5, Ge_2H_6, Ge_3H_6(GeH-Ge_2H_5), Ge_3H_7, Ge_3H_8, Ge_4H_8(GeH-Ge_3H_7), Ge_4H_9, Ge_4H_{10}, Ge_5H_{10}(GeH-Ge_4H_9) Ge_5H_{11}, Ge_5H_{12}, Ge_6H_{12} (hexagonal), and Ge bulk with one interstitial H were employed as references during the fitting procedure. A structurally modified GeH_4 molecule with elongated Ge-H bond lengths and modified angles was also used to account for possible distortion effects. Finally, the frequencies of vibration of GeH_4, GeH_3, GeH_2, and GeH were involved in the fitting procedure to ensure a proper behavior of the second derivative of this potential. Table II reports the obtained parameters. The Ge and H parameters have been taken from the original Tersoff[9] and Murty[10] forms. The cutoff radius (R) of the H-H interaction has been enlarged to 2.0 Å with respect to its original value (1.7 Å) to describe the interactions occurring on a dihydride terminated Ge(100) surface.

C. Parameter validation and discussion

We implemented the Murty and Atwater potential in the XMD molecular dynamic simulation package[25] to gauge the accuracy of the fitted parameters. All the tested models were optimized using a molecular dynamic annealing approach, in which the systems were first heated up to 300 K to be finally slowly cooled down to 0 K.

The comparison of the physical properties obtained between the DFT and the fitted parameter set is listed in Table III. The potential closely reproduces the structure and the averaged binding energies of the saturated Ge hydrides. The deviations of the Ge-H bond length, angle, and binding energies in these H saturated clusters are within ±0.01 Å, $\sim3.0°$, ±0.06 eV, respectively. Even for significantly distorted structures, such as the triangular (Ge_3H_6), squared (Ge_4H_8), and pentagonal (Ge_5H_{10}) clusters, the predicted bond length and binding energy per atom remain within the same error range as the ones mentioned above.

Whenever a germanium bond is unsaturated on the cluster, the presence of the dangling bond induces a local relaxation of the bond lengths (and of their associated binding energies) of the hydrogenated bonds present in the neighboring. This situation is accounted for through the coefficients $F1$, $F2$, and H in the attractive, repulsive, and angular parts of the potential, respectively (which depend on the coordination number N of the host Ge atom). The obtained parametrization reproduces both bond lengths and average binding energies with a similar accuracy as the ones obtained for the

TABLE III. Calculated bond length, binding energy per atoms, bond angle and vibrational frequencies (cm^{-1}) of a set of Ge_nH_m molecules.

	This work	B3LYP		This work	B3LYP		This work	B3LYP
	GeH_4			GeH_3-GeH_3		GeH_2-GeH_3		
$\alpha_{\text{Ge-H}}$(Å)	1.537	1.533	$\alpha_{\text{Ge-H}}$(Å)	1.537	1.537	$\alpha_{\text{Ge-H}}$(Å)	1.539	1.546
E(eV)	2.375	2.378	$\alpha_{\text{Ge-Ge}}$(Å)	2.467	2.445	$\alpha_{\text{Ge-Ge}}$(Å)	2.46	2.45
$\theta_{\text{H-Ge-H}}$	109.5	109.5	E(eV)	2.455	2.424	E(eV)	2.37	2.28
v_1	827.5	827.9	$\theta_{\text{H-Ge-H}}$	108.31	108.48	$\theta_{\text{H-Ge-H}}$	115.45	108.33
v_2	936.7	932.7	$\theta_{\text{H-Ge-Ge}}$	110.60	110.57	$\theta_{\text{H-Ge-Ge}}$	115.47	113.00
v_3	2103.0	2128.9		GeH_3-GeH_2-GeH_3		GeH_2-GeH_2		
v_4	2121.8	2145.7	$\alpha_{\text{Ge-H}}$(Å)	1.537	1.541	$\alpha_{\text{Ge-H}}$(Å)	1.539	1.544
	GeH_3		$\alpha_{\text{Ge-Ge}}$(Å)	2.467	2.450	$\alpha_{\text{Ge-Ge}}$(Å)	2.45	2.306
$\alpha_{\text{Ge-H}}$(Å)	1.539	1.540	E(eV)	2.493	2.449	E(eV)	2.26	2.24
E(eV)	2.175	2.079	$\theta_{\text{H-Ge-H}}$	107.46	107.32	$\theta_{\text{H-Ge-H}}$	115.39	107.83
$\theta_{\text{H-Ge-H}}$	115.45	110.81	$\theta_{\text{H-Ge-Ge}}$	110.41	109.12	$\theta_{\text{H-Ge-Ge}}$	115.41	115.55
v_1	852.3	863.6		GeH_3-GeH-GeH_3-GeH_3		GeH-GeH_2		
v_2	2080.5	2046.5	$\alpha_{\text{Ge-H}}$(Å)	1.536	1.544	$\alpha_{\text{Ge-H}}$(Å)	1.562,	1.598,
v_3	2099.0	2111.8	$\alpha_{\text{Ge-Ge}}$(Å)	2.464	2.455		1.539	1.549
GeH_2			E(eV)	2.52	2.46	$\alpha_{\text{Ge-Ge}}$(Å)	2.46	2.44
$\alpha_{\text{Ge-H}}$(Å)	1.562	1.604	$\theta_{\text{H-Ge-H}}$	108.10	108.48	E(eV)	2.16	2.12
E(eV)	2.029	1.951	$\theta_{\text{H-Ge-Ge}}$	110.31	107.79	$\theta_{\text{H-Ge-H}}$	115.44	105.94
$\theta_{\text{H-Ge-H}}$	88.01	90.86		Ge_6H_{12}(Hexagonal)			115.44,	123.74,
v_1	843.5	936.1	$\alpha_{\text{Ge-H}}$(Å)	1.537	1.541	$\theta_{\text{H-Ge-Ge}}$	88.01	88.075
v_2	2142.9	1887.9	$\alpha_{\text{Ge-Ge}}$(Å)	2.466	2.458	GeH-GeH		
GeH			E(eV)	2.59	2.51	$\alpha_{\text{Ge-H}}$(Å)	1.562	1.586
$\alpha_{\text{Ge-H}}$(Å)	1.594	1.604	$\theta_{\text{H-Ge-H}}$	107.38	107.55	$\alpha_{\text{Ge-Ge}}$(Å)	2.442	2.446
E(eV)	1.41	1.44	$\theta_{\text{H-Ge-Ge}}$	110.35	108.77	E(eV)	2.012	1.927
v_1	2062.8	1922.6				$\theta_{\text{H-Ge-Ge}}$	88.01	103.65

saturated Ge hydrides (Table III). When two H atoms are removed from the same Ge site, the electrostatic repulsion of the generated dangling bonds is such that the molecule adopts a 90° H-Ge-Ge conformation. The latter is also properly described by our parameter set, with some minor deviations with respect to the DFT results.

The frequencies of vibration of the Ge-H bonds are associated to the second derivate of the interatomic potential. The Ge-H potential reproduces correctly the DFT outcomes obtained for the different vibration modes of the Ge hydrides. Note however that the deviations of the phonon frequencies obtained with the Ge-H potential with respect to the DFT values are on the same order of magnitude than the ones reported by Murty and Atwater[10] with their Si-H potential. Yet, our parameter set offers a lower deviation with respect to the DFT values for the GeH_3 and GeH_4 molecules than the one proposed by Murty and Atwater for their silicon homologous.

For the cluster radicals associated with a double bond, such as GeH_2-GeH_2, GeH_2-GeH, and GeH-GeH, the potential describes with a lower accuracy on the angular dependence and leads to bond angle deviations ranging from $\sim 10°$ to 20° compared to DFT. This deviation finds its origin into the analytical formulation developed by Tersoff (Murty and Atwater): the binding conditions of the neighboring Ge atoms are not taken into account; the double bonds are then regarded as normal Ge-Ge ones.

The transferability of our parameters has also been tested on a 2×1 Ge(100) surface for different surface hydrogen coverage. A clean Ge(100) surface exhibits a 2×1 reconstruction with the surface dimer bond along the $\langle 110 \rangle$ direction. For a hydrogen coverage of 1 AL, the dangling bonds are passivated and the hydrogen terminated structure preserves its 2×1 reconstruction [Fig. 2(a)]. The computed Ge-Ge dimer bond length (2.53 Å) and their associated H-Ge-H bond angles (113.2°) are found to be similar to the DFT values of 2.53 Å and 109.7°. Upon the deposition of 2 AL, a strong repulsion occurs between the H atoms present on the hydrogenated dimer and the other neighboring dihydrides; the surface recovers its (1×1) topology, which results into a canted-row structure [Fig. 2(b)]. The R cutoff value proposed by Murty and Atwater[10] for the H is too small to properly account for this long-range interaction in the germanium-hydrogen case. We found that increasing its value from 1.7 to 2.0 Å is enough to reproduce the steric hindrance effect. Similarly to what has been calculated from DFT [Fig. 2(b)], the strong repulsion which occurs between the neighboring H atoms leads to a tilt of the surface germanium atoms.

Next, we consider the case of interstitial hydrogen in bulk germanium and assess the structures and the energetic ob-

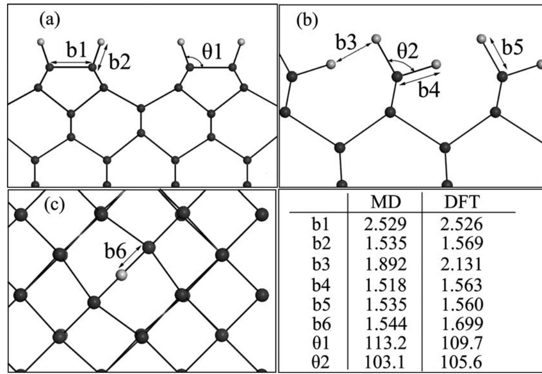

	MD	DFT
b1	2.529	2.526
b2	1.535	1.569
b3	1.892	2.131
b4	1.518	1.563
b5	1.535	1.560
b6	1.544	1.699
θ1	113.2	109.7
θ2	103.1	105.6

FIG. 2. Illustration of the topologies obtained for the H terminated Ge surface [(a) monohydride, (b) dyhidride, and (c) H interstitial structure]. The germanium and hydrogen atoms are represented in black and gray, respectively.

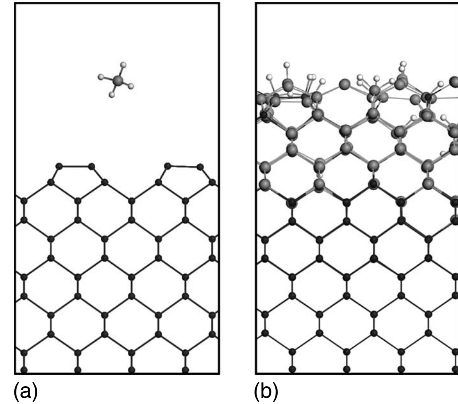

FIG. 3. Illustration of the (a) initial and (b) final configurations obtained for the epitaxial growth of 5 AL of Si on Ge(100). The black small dots correspond to the Ge atoms and the large gray ones to the Si ones. The H atoms are represented by the small gray dots.

tained with DFT and the fitted potential for a periodic unit cell made of 64 Ge atoms and an interstitial H atom. The configuration of a bond-centered interstitial H was included into the references used in our fitting work. From a structural point of view, the fitted potential reproduces the DFT results; the Ge-Ge bonds around the inserted H atom are distorted to accommodate the presence of the extra hydrogen atom [Fig. 2(c)]. The binding energy of the inserted H atom generated with the analytical potential is however underestimated by ~ 1.4 eV with respect to the DFT value (2.06 eV). The origin of this discrepancy arises from the difficulty of discerning, during the fitting procedure, bulk interstitial H from H atoms inserted in typical bridged surface topologies such as GeH_3-H-GeH_3. Several attempts have been made to correct the obtained binding energy, but all of them lead to an unrealistic stabilization of the surface bridged Ge-H-Ge structure. Since we target developing a set of parameters dedicated to the simulation of a CVD process, we mainly focused on the H interplay with the surface Si and Ge atoms, sacrificing the accuracy of the description of interstitial hydrogen in Ge bulk phase. The unrealistic stabilization of the surface H bridged conformation contaminates the quality of the results obtained. We therefore reduced the weight of the contribution of the binding energy of the hydrogen bulk interstitial scenario in the fitting procedure to ensure a proper description of the potential for the surface H bridged case.

III. SURFACE SEGREGATION MODELING

The segregation of Ge at the surface during the epitaxial growth of Si on a Ge(100) buffer is a technological issue that compromises the role of Si as an electrical passivation layer for germanium. Previous works have been focusing on the mechanisms at the origin of the germanium up-diffusion, especially on the quantification of the energy barriers for the elementary germanium diffusion processes.[6] Here, we consider the phenomenon in its entirety: by combining our fitted Ge-H parameters with the Murty and Atwater[10] Si-H one, we simulated the CVD growth of Si on a Ge(100) surface starting from SiH_4 precursors.

A. Simulation of the CVD of Si growth on Ge(100)

The initial configuration of our model consists in a squared supercell made of 32 (2×1) reconstructed Ge(100) units with a thickness of 12 AL of Ge [Fig. 3(a)]. To mimic the bulk behavior of germanium, the bottom two layers of the slab were kept fixed and the next two ones were maintained in a constant-temperature bath of 820 K using the velocity scaling method.[26] During the deposition process, the SiH_4 molecules randomly appear in the upper space of the Ge buffer layer and bombard the surface. To be able to simulate the CVD process within a reasonable simulation time scale, enough SiH_4 molecules have to be cracked on the surface. However, the stochastic character of the collisions makes the process too slow to occur within a MD time frame. To solve this problem, we followed the procedure described in Refs. 27 and 28 that consists in increasing the kinetic energy of the precursor SiH_4 molecules (and therefore their sticking coefficients). As a kinetic energy, we chose a value of 3.07 eV, close to the binding energy of Si-H in the SiH_4 molecule [3.4 eV (Ref. 10)].

In this work, 5 AL of Si were grown on top of Ge(100) using two different approaches to reproduce the factors that drive the surface segregation mechanism of Ge on Si.[5] In the first one, the Si epitaxial layers were grown layer by layer. The growth of each AL of Si is a process of combined deposition and annealing treatments: the surface is first bombarded by SiH_4 molecules with a time interval of 4 ps (5000 MD time steps) between two collisions. Once a complete atomic layer of Si is deposited, a thermal annealing treatment (at 2200 K) is performed during 22.4 ns $(2.8\times 10^7$ MD steps). Note that the H atoms are manually removed from the surface before the application of the thermal annealing to account for the hydrogen desorption process that occurs beyond 773 K. This thermal procedure accelerates the surface diffusion events (see below for further details) which otherwise would not be accessible within our simulation time scale. The temperature (2200 K) has been carefully chosen to prevent the melting of the substrate while keeping the surface diffusion active.

After five cycling steps, leading to the bombardment of 12×10^3 SiH_4 molecules on the surface and a total of 112 ns

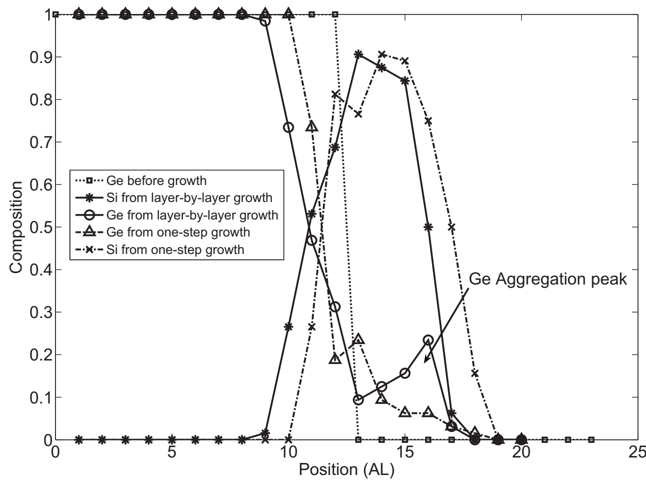

FIG. 4. Distribution of the Si(Ge) content in the system for 5 AL of Si deposited on Ge(100) using two different approaches. A Ge segregation peak is observed during the layer-by-layer growth but not during the one-step one.

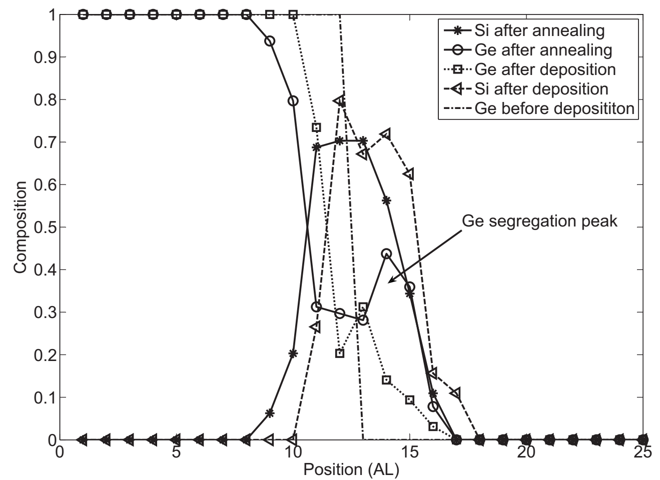

FIG. 6. Distribution of the Si(Ge) content in the film for 3 AL of Si deposited on Ge(100) in the one-step approach. The dashed and dotted lines correspond to the composition in Si and Ge after the deposition of Si and the solid ones, to the situation after annealing.

of thermal annealing, 5 AL of Si were grown epitaxially on the Ge surface. During the deposition, germanium up diffuses in the silicon layers to segregate close to the Si surface (see Fig. 4). The driving force of the process arises from the difference in surface energies between Si and Ge; the segregation of Ge at the Si surface leads to a stabilization of the surface by about 0.4 eV per Ge dimer created compared to the nonsegregated case.

The composition of the surface after the deposition of each AL of Si has been monitored (Fig. 5). The profile correlates nicely with the experimental time-of-flight secondary ion mass spectroscopy (TOFSIMS) measurements recently reported by Caymax *et al.*[29] for the deposition of SiH_4 on Ge(100). Note that our simulations predict a somewhat lower surface concentration of Ge than what is observed experimentally. We speculate that the origin of this discrepancy arises from the desorption of Ge during the deposition process. Indeed, the continuous supply of hydrogen from the cracked SiH_4 molecules combined with the dissipation of the kinetic energy of the bombarding SiH_4 molecules is enough to initiate the desorption of Ge atoms from the surface as Ge hydrides.

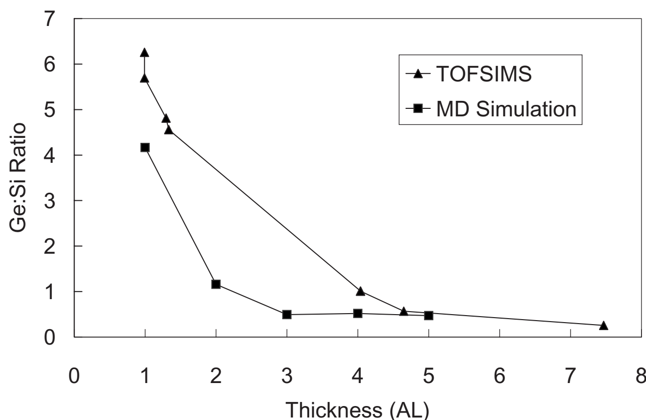

FIG. 5. Comparison of the Ge:Si surface ratio obtained from the simulated CVD process (square) and TOFSIMS data (triangle).

In the second approach, we bombarded the surface with SiH_4 molecules and neglected the thermal treatment steps until 5 AL of Si are deposited on the surface. In this "one-step growth" approach, we imposed a time interval between two SiH_4 collisions of 8 ps (i.e., 10^4 MD time steps). Although the temperature of the substrate is kept at 820 K, many H atoms remain chemisorbed on the Si surface [Fig. 3(b)] and saturate the dangling bonds. This source of H finds its origin in the combination of the relatively short simulation time and in the cracking of the SiH_4 molecules. This therefore does not allow a complete desorption of the H atoms, which typically requires a longer simulation time scale to occur. The incoming SiH_4 molecules are absorbed on the surface through the collision with the Si-H or Ge-H bonds. Interestingly, the composition profile (Fig. 4 one-step growth) reveals a lower segregation of Ge on the Si surface compared to the "layer-by-layer" approach, which suggests that the saturation of the surface by the remaining hydrogen atoms has an impact on the Ge surface segregation mechanism.

B. Ge up-diffusion through surface defects

The analysis of the film topology obtained after deposition reveals the presence of numerous surface defects such as voids, adatoms, islands, and steps. The intermixing between the Si adatoms and the surface Ge ones is believed to be at the origin of the low energy pathway for the Ge surface segregation.[6] When the Si epitaxial layer is very thin (1 $\sim$3 AL), the surface defects open extra channels for the bulk Ge atoms to interact with the Si adatoms, which ends to a stronger Ge segregation. We investigated this scenario by subsequently annealing the "one-step" model with 3 AL of Si, while removing the surface H. After a thermal treatment of 67 ns, a strong segregation of Ge occurs close to the surface (Fig. 6): dimers are formed upon the reconstruction of the diffused atoms with the vacant sites, which leads to the reduction of the surface steps. The contribution of the dif-

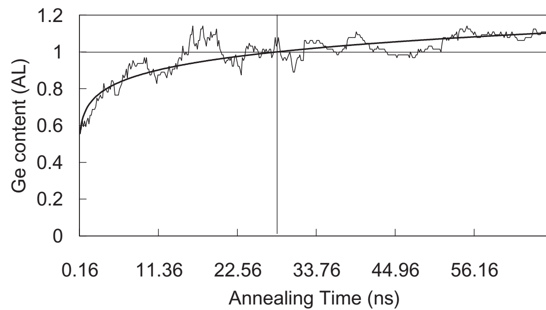

FIG. 7. Evolution of the Ge content in the Si epitaxial layer during the annealing of a thin ($\sim\pi 3$ AL) Si layer on Ge(100), the black thicker line illustrates the general trend obtained for the Ge aggregation.

fused Ge atoms in the epitaxial layer is nicely illustrated when monitoring the evolution of the Ge content in the epitaxial layer during the thermal treatment (Fig. 7). It should be pointed out that each point of Fig. 7 has been extracted from the relaxed epitaxial structure cooled down at 0 K to eliminate any artifacts in the monitoring of the Ge content.

In a first step, Ge rapidly diffuses to the surface to compensate its defects and to dimerize with the available neighbors. After 28 ns of thermal treatment, the Ge content in the epitaxial layer reaches 1 AL; its diffusion is slowed down and the surface became smoother. The saturation of Ge in the deposited layer decreases the potential-energy difference, which in turn, reduces the driving force for diffusion.

C. Discussion of the surface segregation

The comparison of the energetic between the Si capped structures and the Ge segregated ones demonstrates opposite trends upon the H passivation. The presence of H stabilizes the Si capped structure by about 0.18 eV per surface dimer compared to the Ge segregated model (in which the Si layer is buried in the bulk of the layers). Upon the removal of the surface H atoms, the situation gets reversed: the reconstructed Ge segregated surface becomes energetically more stable by 0.4 eV per dimer with respect to the Si terminated one. These numbers are qualitatively consistent with the ones reported for similar surface topologies (0.08 and 0.38 eV) by Cakmak and Srivastava[8] using first-principles simulations.

In the "one-step" approach, the continuous supply of H atoms during the cracking of the SiH_4 molecules maintains the surface passivated, which hence favors the segregation of Si. However, the calculated growth rate of the Si film is 8 mm/s, which is much faster than what is obtained in typical experimental conditions [about 83 nm/s at 773 K (Ref. 5)]. This difference finds its origin in the larger kinetic energy provided to the SiH_4 molecules with respect to the normal gas phase conditions met in a CVD reactor. This is however a necessity to maintain the simulation time scale computationally tractable. Such a high growth rate might take over the relative slow Ge up-diffusion processes and hence reduces the Ge segregation. Still, in our simulation, the temperature bath at 820 K is concentrated on the lower third and forth Ge layers, which are buried far from the surface. Upon the collision, the dissipation of the kinetic energy of the SiH_4 molecules heats the surface and accelerates the diffusion mechanisms. Therefore, the reduction in the Ge segregation is believed to be representative of the physical process related to the difference in surface energies due to the H termination.

Similarly, in the "layer-by-layer" growth approach and upon the removal of the H atoms from the surface, the use of a high temperature is needed to activate the Ge diffusion during the annealing. This is consistent with the low-energy barrier (1.5 eV) reported by Boguslawski and Bernholc[6] for the diffusion of Ge in absence of H. Assuming that the diffusion is associated with an attempt frequency factor of $\sim 10^{13}$ Hz at 820 K, the process requires $\sim 10^{-4}$ s to occur. Within the framework of classical molecular dynamics, this time window is unfortunately not accessible and is about 5 orders of magnitude longer than what can be handled with our computational resources. When the temperature is increased to 2200 K, the time needed for such a diffusion process to occur is reduced to $\sim 10^{-9}$ s, which allows the phenomenon to happen during our thermal treatment of the film.

In absence of H chemisorbed at the surface, a strong surface Ge segregation occurs through concerted exchange mechanisms between the Si or Ge atoms at flat terrace, step-edge or adatom sites.[6] This suggests that the rougher the surface, the stronger the Ge segregation. The annealing treatment of the 3 AL Si layers leads to the stabilization of the surface reconstruction by the formation of dimers between the surface atoms, which reduces the number of abrupt steps and voids. This, together with the saturation of Ge in the epitaxial layer, is expected to lessen the driving force of the Ge segregation.

IV. CONCLUSIONS

A parameter set for a Tersoff-based Ge-H interaction potential has been derived from first-principles calculations. The obtained parametrization displays a good adaptability and transferability for both germanium- and hydrogen-based molecules, frequency of vibrations, and surface properties. Using this potential, the mechanisms of the CVD growth of an epitaxial silicon on a Ge(100) surface using a silane gas source have been simulated. Our molecular-dynamics simulations demonstrate that the surface Si(Ge) segregation occurring during the Si deposition is driven by the presence of chemisorbed hydrogen that governs the changes in surface energy between Si and Ge. The latter prevents the diffusion of Ge toward the surface of the deposited silicon films. These results are consistent with recent experimental reports and TOFSIMS profiles.[5,29] This therefore suggests that the proposed Ge-H parameter set is suitable for the simulation of physical processes occurring during the film growth.

[1] C. O. Chui, H. Kim, D. Chi, P. C. McIntyre, and K. C. Saraswat, IEEE Trans. Electron Devices **53**, 1509 (2006).
[2] M. Caymax, S. Van Elshocht, M. Houssa, A. Delabie, T. Conard, M. Meuris, M. M. Heyns, A. Dimoulas, S. Spiga, M. Fanciulli, J. W. Seo, and L. V. Goncharova, Mater. Sci. Eng., B **135**, 256 (2006).
[3] *Germanium Based Technologies: From Materials to Devices*, edited by C. Claeys and E. Simoen (Elsevier, New York, 2007).
[4] P. Zimmerman, G. Nicholas, B. De Jaeger, B. Kaczer, A. Stesmans, L-A. Ragnarsson, D. P. Brunco, F. E. Leys, M. Caymax, G. Winderickx, K. Opsomer, M. Meuris, and M. M. Heyns, Tech. Dig. - Int. Electron Devices Meet. **655**, 1 (2006).
[5] F. E. Leys, R. Bonzom, B. Kaczer, T. Janssens, W. Vandervorst, B. De Jaeger, J. Van Steenbergen, K. Martens, D. Hellin, J. Rip, G. Dilliway, A. Delabie, P. Zimmerman, M. Houssa, A. Theuwis, R. Loo, M. Meuris, M. Caymax, and M. M. Heyns, Mater. Sci. Semicond. Process. **9**, 679 (2006).
[6] P. Boguslawski and J. Bernholc, Phys. Rev. Lett. **88**, 166101 (2002).
[7] K. Sumitomo, K. Shiraishi, Y. Kobayashi, T. Ito, and T. Ogino, Thin Solid Films **357**, 76 (1999).
[8] M. Çakmak, S. C. A. Gay, and G. P. Srivastava, Surf. Sci. **454-456**, 166 (2000).
[9] J. Tersoff, Phys. Rev. B **39**, 5566 (1989).
[10] M. V. Ramana Murty and H. A. Atwater, Phys. Rev. B **51**, 4889 (1995).
[11] C. V. Ciobanu and R. M. Briggs, Appl. Phys. Lett. **88**, 133125 (2006).
[12] A. J. Dyson and P. V. Smith, Mol. Phys. **96**, 1491 (1999).
[13] A. V. Nemukhin, B. L. Grigorenko, and A. A. Granovsky, Moscow Univ. Chem. Bull. (Engl. Transl.) **45**, 75 (2004).
[14] J. H. Callomon, E. Hirota, K. Kuchitsu, W. J. Lafferty, A. G. Maki, and C. S. Pote, *Structure Data of Free Polyatomic Molecules* (Springer, Berlin, 1976).
[15] R. C. Binning and L. A. Curtiss, J. Chem. Phys. **92**, 1860 (1990).
[16] K. Balasubramanian, J. Chem. Phys. **89**, 5731 (1988).
[17] K. Huber and G. Herzberg, *Molecular Spectra and Molecular Structure 4. Constants of Diatomic Molecules* (Van Nostrand, Princeton, 1979).
[18] T. Shimanouchi, *Tables of Molecular Vibrational Frequencies*, National Standard Reference Data Series, National Bureau of Standards (U.S. GPO, Washington, D.C., 1972), Vol. 39.
[19] G. R. Smith and W. A. Guillory, J. Chem. Phys. **56**, 1423 (1972).
[20] J. M. Soler, E. Artacho, J. D. Gale, A. Garcia, J. Junquera, P. Ordejon, and D. Sanchez-Portal, J. Phys.: Condens. Matter **14**, 2745 (2002).
[21] N. Troullier and J. L. Martins, Phys. Rev. B **43**, 1993 (1991).
[22] J. Junquera, O. Paz, D. Sanchez-Portal, and E. Artacho, Phys. Rev. B **64**, 235111 (2001).
[23] X. Gonze, J.-M. Beuken, R. Caracas, F. Detraux, M. Fuchs, G.-M. Rignanese, L. Sindic, M. Verstraete, G. Zerah, F. Jollet, M. Torrent, A. Roy, M. Mikami, Ph. Ghosez, J.-Y. Raty, and D. C. Allan, Comput. Mater. Sci. **25**, 478 (2002).
[24] A. Corana, M. Marchesi, C. Martini, and S. Ridella, ACM Trans. Math. Softw. **13**, 262 (1987).
[25] http://xmd.sourceforge.net/.
[26] L. V. Woodcock, Chem. Phys. Lett. **10**, 257 (1971).
[27] T. A. Plaisted and S. B. Sinnott, J. Vac. Sci. Technol. A **19**, 262 (2001).
[28] M. E. Taylor, H. A. Atwater, and M. V. Ramana Murty, Thin Solid Films **324**, 85 (1998).
[29] M. Caymax, J. Mitard, K. Martens, L. Yang, G. Pourtois, W. Vandervorst, and M. Meuris, Si Passivation in Ge *p*MOSFETS: Further Developments and Understanding, invited presentation at the 4th International WorkShop on New Group IV Semiconductor Nanoelectronics, Tohoku University, Sendai, Japan, Sept. 25–27, 2008 (unpublished).